Nanoscale

PAPER

View Article Online
View Journal | View Issue

Cite this: *Nanoscale*, 2015, **7**, 6836

Amino-functionalized green fluorescent carbon dots as surface energy transfer biosensors for hyaluronidase†

Siyu Liu,[a] Ning Zhao,[a] Zhen Cheng*[b] and Hongguang Liu*[a]

Received 6th January 2015,
Accepted 18th March 2015

DOI: 10.1039/c5nr00070j

www.rsc.org/nanoscale

Amino-functionalized fluorescent carbon dots have been prepared by hydrothermal treatment of glucosamine with excess pyrophosphate. The produced carbon dots showed stabilized green emission fluorescence at various excitation wavelengths and pH environments. Herein, we demonstrate the surface energy transfer between the amino-functionalized carbon dots and negatively charged hyaluronate stabilized gold nanoparticles. Hyaluronidase can degrade hyaluronate and break down the hyaluronate stabilized gold nanoparticles to inhibit the surface energy transfer. The developed fluorescent carbon dot/gold nanoparticle system can be utilized as a biosensor for sensitive and selective detection of hyaluronidase by two modes which include fluorescence measurements and colorimetric analysis.

Introduction

Fluorescent nanomaterials have attracted considerable attention in biomedical fields including bioimaging, drug delivery and biosensing because of their small size, long fluorescence lifetime, tunable fluorescence emission and high photostability.[1,2] In the development of fluorescent nanomaterials, studies on the applications of quantum dots (QDs) hold an important position.[3] However, the leakage of heavy metal elements such as cadmium, lead, mercury and silver resulting in cytotoxicity and environmental pollution severely hampers QDs' applications.[4] Recently, fluorescent carbon dots (CDs) have been proposed as a class of promising and less toxic nanomaterials to replace traditional QDs.[5]

Since Sun and co-workers first reported nanoscale bright photoluminescence carbon nanoparticles upon simple surface passivation,[6] fluorescent CDs have shown attractive properties for their use in bioimaging and biosensing due to their high photostability, excellent cell membrane permeability, water solubility and biocompatibility.[7] So far, a series of synthesis methods for fluorescent CDs have been developed. One approach is to produce carbon nanotubes or soot of candles from larger carbon sources through laser irradiation, and electrochemical and chemical oxidation of graphite.[8] The other approach is to synthesize fluorescent CDs from carbon precursors such as glycerol, glycol, glucose, sucrose, citric acid, *etc.* through chemical and hydrothermal oxidation or microwave pyrolysis.[9] However, most of these methods usually need complex procedures or modifications to improve the surface state of the CDs. The amino-group functionalization could effectively increase the biocompatibility and hydrophilicity of CDs and make it easy for further modifications.[10a] But the surface modification using amine-terminated compounds are complex and time-consuming.[10b] Yang *et al.* proposed a method to prepare amino-functionalized fluorescent CDs by hydrothermal carbonization of chitosan,[10c] but the poor water solubility of chitosan and highly acidic synthetic environment restricted its broad applications. Herein, we report a one-pot synthetic route to prepare water-soluble amino-functionalized CDs through hydrothermal treatment of glucosamine in excess pyrophosphate solution, and we further use it for imaging biomarkers such as hyaluronidase (Hase).

Hase is an extracellular matrix digesting endoglycosidase and can degrade hyaluronate (HA), which is a highly negatively charged linear mucopolysaccharide.[11] Hase is involved in a variety of physiological and pathological processes including fertilization, embryogenesis, maintenance of the elastoviscosity in tissues, wound healing, inflammation, and tumor growth.[12] In recent years, the changes in the Hase level in human blood and urine have been found to be associated with the growth of numerous human tumors such as bladder cancer and prostate cancer.[13] Therefore, to develop a highly sensitive and specific technique for the detection of the Hase level is important and desired. Until now, a series of fluorescent labeled substrates including HA have been designed

[a]*Institute of Molecular Medicine, College of Life and Health Sciences, Northeastern University, Shenyang 110000, China. E-mail: simonliu@mail.neu.edu.cn*
[b]*Molecular Imaging Program at Stanford, Stanford University, Palo Alto, CA 94301, USA. E-mail: zcheng@stanford.edu*
†Electronic supplementary information (ESI) available. See DOI: 10.1039/c5nr00070j

for sensitive and real-time monitoring of the Hase level.[14,15] For instance, Chib *et al.* used a HA probe labeled with fluorescein as a donor and rhodamine as an acceptor to monitor the digestion of the HA probe with different concentrations of Hase in synthetic urine *via* fluorescence emission.[15a] Fluorescent CDs, as novel fluorescent nanosensors, have been utilized to detect a variety of biological molecules and stimuli such as Hg^{2+}, Pb^{2+}, Ag^{+}, DNA, glucose, tissue pH based on fluorescence changes.[16,17] However, the reports on fluorescent CD-based nanosensors for enzyme assay are very rare.

Gold nanoparticles (Au NPs), as a kind of nanomaterial, possess strong light scattering and absorption ability, and a large surface-to-volume ratio. The surface of Au NP follows the expression given by surface energy transfer (SET) that allows a 22 nm detection length scale instead of a 10 nm detection length in fluorescence resonance energy transfer.[18] Because of the highly sensitive fluorescence quenching ability of Au NPs, the novel SET process possesses great potential for target detection and molecular interaction studies.[18c] In this work, we first designed a facile SET system between the positively charged amino-functionalized carbon dots and negatively charged hyaluronate stabilized gold nanoparticles (HA-Au NPs) for the detection of Hase based on its ability to degrade HA. Moreover, the Hase level changes can be monitored simultaneously by the fluorescence emission intensity and visible light absorption values of the CD/HA-Au NP SET assay system.

Experimental section

Apparatus

The fluorescence spectra were recorded using a Thermo Scientific Lumina fluorescence spectrometer with a xenon lamp using right-angle geometry. UV-Vis absorption spectra were recorded by using a Biotek Synergy™ H1 microplate reader. FT-IR spectra were recorded using a Bruker IFS66 V FT-IR spectrometer equipped with a DGTS detector (32 scans). Transmission electron microscopy (TEM) experiments were performed using a Philips Tecnai F20 TEM operating at 200 kV acceleration voltage. TEM samples were prepared by dropping the aqueous fluorescent CDs or HA-Au NP solution onto carbon-coated copper grids and allowing the excess solvent to evaporate.

Chemicals and materials

All reagents were of at least analytical grade. The water used in all experiments had a resistivity higher than 18 MΩ cm^{-1}. Potassium phosphate (K_3PO_4), sodium phosphate (Na_3PO_4), sodium hydrogen phosphate (Na_2HPO_4), sodium dihydrogen phosphate (NaH_2PO_4), sodium pyrophosphate ($Na_4P_2O_7$), sodium triphosphate ($Na_5P_3O_{10}$), and sodium hexametaphosphate (Na_6P_{6O18}) were purchased from Sinopharm Chemical Reagent Co., Ltd. D-Glucosamine hydrochloride, sodium borohydride ($NaBH_4$), chloroauric acid ($HAuCl_4$), sodium hyaluronate, Hase (400 U mg^{-1}), fetal bovine serum and dialysis tubing cellulose membrane (3 kDa) were purchased from Sigma-Aldrich Corporation.

Synthesis of amino-functionalized fluorescent CDs

In a typical synthetic route, amino-functionalized fluorescent CDs were prepared as follows: 1 mL of 75 mmol per L D-glucosamine hydrochloride solution was added to 14 mL of deionized water solution containing 0.938 mmol sodium pyrophosphate, with vigorous stirring at room temperature. After 10 minutes, the solution was transferred into a Teflon lined stainless steel autoclave with a volume of 25 mL. The autoclave was maintained at 180 °C for 10 h and then cooled down to room temperature by a natural cooling process. The obtained yellow-brown CD solution was centrifuged at a speed of 12 000 rpm at 4 °C for 40 min to remove the black deposit and excess sodium pyrophosphate. The upper yellow-brown solution was dialyzed in the membrane tubing with a molecular weight cut-off of 3 kDa against ultrapure water to remove small molecules and ions and then stored at 4 °C. The purified CD solution was freeze-dried into a powder, and the concentration of the amino-functionalized fluorescent CDs in solution was about 2.1 mg mL^{-1} as measured by the dry weight analysis method.

Synthesis of HA-Au NPs

The HA-Au NPs were synthesized according to the previous reports with some modifications.[18d,19] In a typical synthetic process, HA-Au NPs were prepared as follows: 1 mL of $HAuCl_4$ (0.12 mol L^{-1}) solution was added into 50 mL 0.01% (w/v) sodium hyaluronate aqueous solution with vigorous stirring for 20 minutes at room temperature. After that, 1 mL of $NaBH_4$ (4 mg mL^{-1}) was slowly injected into the above solution, and the color of the solution changed from yellow to red purple indicating the formation of significant amounts of HA-Au NPs. The reaction was allowed to proceed for another 5 minutes under vigorous stirring. After that the product was purified to remove small molecules and ions *via* ultra-filtration (10 kDa ultra-filtration centrifuge tube) and dissolved in deionized water again. The purified HA-Au NP solution was stored at 4 °C.

The SET system for the detection of Hase

The Hase detection process was carried out as follows: 20 μL 0.1 mol per L NaH_2PO_4–Na_2HPO_4 buffer solution (pH 6.0), 20 μL CD solution (0.21 mg mL^{-1}), 20 μL HA-Au NPs and different concentrations of Hase were respectively added into a 200 μL calibrated centrifuge tube. Then the solution was diluted to 200 μL with deionized water followed by incubation at 37 °C for 2 hours. The fluorescence emission and UV-Vis absorption spectra were recorded and used for quantitative analysis.

Quantum yield measurements

The quantum yield (QY) of CDs was determined by comparing it with a reference fluorophore. Fluorescein (QY_R = 0.79) was used as the reference fluorophore for the determination of QY.

For obtaining a standard measurement, the fluorescein was dissolved in 0.1 mol per L NaOH (refractive index n = 1.33), and CDs were dispersed in deionized water (n = 1.33). Then the quantum yield was calculated by the following equation:

$$QY = QY_R \times (I/I_R) \times (A_R/A) \times (n^2/n_R^2)$$

where I is the integrated fluorescence emission intensity, A is the absorbance intensity and n is the refractive index. The subscript R refers to the reference fluorophore of the known quantum yield.

Results and discussion

The preparation and characterization of amino-functionalized CDs

In the present work, we proposed a one-pot green route to prepare green-emitting amino-functionalized CDs and then adopted the synthesized CDs as a new type of selective and sensitive biosensor for the detection of Hase based on the SET system (Scheme 1). As shown in Scheme 1A which displays a typical CD synthesis, pyrophosphate and glucosamine, which are important nutrients in human chondrocytes, were dissolved in aqueous solution at room temperature. When the reaction mixture was heated from room temperature to 180 °C, the colorless transparent reaction solution turned yellow brown and produced a highly green fluorescent product under ultraviolet light. In the synthetic process, glucosamine was adopted as a natural nitrogen-doped carbon source, and sodium pyrophosphate was used as a catalytic agent.[9]

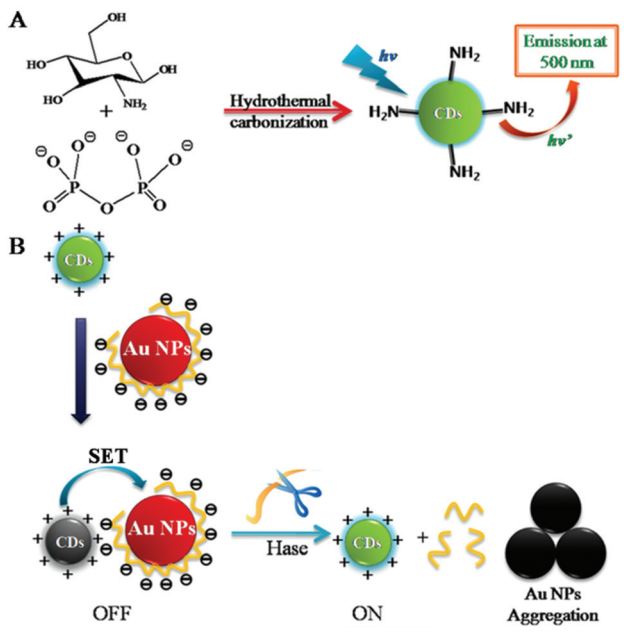

Scheme 1 (A) The schematic illustration of the synthetic process of amino-functionalized CDs and (B) the use of prepared CDs and Au NPs as a SET biosensor system for Hase.

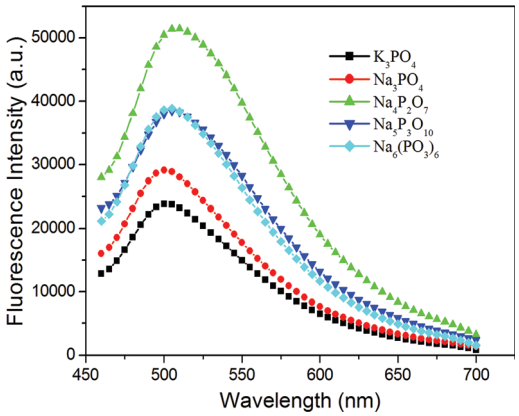

Fig. 1 Fluorescence emission spectra of CDs excited at 420 nm obtained using polyphosphates such as potassium phosphate (125 mmol L^{-1}), sodium phosphate (125 mmol L^{-1}), sodium pyrophosphate (62.5 mmol L^{-1}), sodium triphosphate (41.7 mmol L^{-1}) or sodium hexametaphosphate (20.8 mmol L^{-1}).

In previous reports, nitric acid, chlorosulfonic acid or phosphoric acid was utilized as the oxidizing agent or the catalytic agent during the synthesis of CDs.[8,9] Here, we have firstly reported the use of sodium pyrophosphate for the preparation of CDs. Fig. 1 shows the fluorescence emission spectra of amino-functionalized CDs prepared with potassium phosphate, sodium phosphate, sodium pyrophosphate, sodium triphosphate or sodium hexametaphosphate. It is observed that the polyphosphates show better results for inducing highly fluorescent CDs than monophosphates; a highly fluorescent emission peak around 500 nm belonging to CDs was also observed with excess sodium pyrophosphate as the catalytic agent. Moreover, Fig. 2 shows the fluorescence changes of the prepared CD solutions.

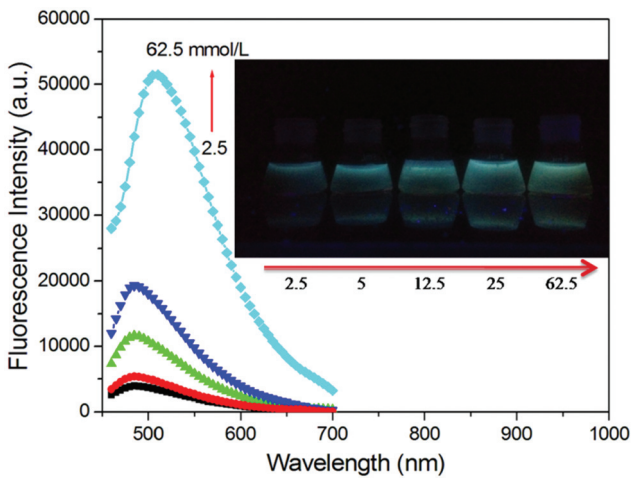

Fig. 2 Fluorescence emission spectra of CDs synthesized by using different concentrations of sodium pyrophosphate increasing from 2.5 to 62.5 mmol L^{-1} (2.5, 5, 12.5, 25, 62.5 mmol L^{-1}). The inset picture shows the color change of the CD solutions synthesized with different concentrations of sodium pyrophosphate under a UV beam of 365 nm.

CD solution with different concentrations of sodium pyrophosphate. When the pyrophosphate concentration just reached 2.5 mmol L^{-1}, the synthesized CD solution showed a very weak green emission fluorescence signal and there were some black deposits at the bottom of the original CD solution. With the pyrophosphate concentration increasing from 2.5 to 62.5 mmol L^{-1}, the fluorescence intensity of CDs enhanced significantly with an increase of QYs from 0.5 to 16.8%. At 62.5 mmol per L pyrophosphate concentration, the prepared CD solution offered maximum fluorescence emission and QY (16.8%). A red-shift of fluorescence emission wavelength (from 480 to 500 nm) with the increase of pyrophosphate concentration was also observed, which corresponded to the size growth of fluorescent CDs.[20a] At the same time, with the increase of pyrophosphate concentration, the black deposit at the bottom of the original CD solution significantly reduced, which further indicates that pyrophosphate effectively prevented carbon nuclei from growing and assembling into large carbon particles during the hydrothermal carbonization.[20] The changing trends of UV-Vis absorption spectra attributed to the CD solution with progressively increasing pyrophosphate concentration were also consistent with their fluorescence spectra (Fig. S1A, ESI†). Furthermore, the enhanced fluorescence emission signal of the CD solution with increasing pyrophosphate concentration could be directly observed by the naked-eye under a UV beam of 365 nm (Fig. 2 inset). It is generally known that the fluorescence emission of CDs arises from the radiative recombination of the excitons trapped by the surface defects that are produced in the passivated procedure.[10c] So far, most of the prepared fluorescent CDs show a similar phenomenon with respect to their emission spectra which are highly dependent on the excitation wavelengths.[8–10] These prepared CDs usually exhibit blue photoluminescence under ultraviolet light excitation. However, as shown in Fig. 2 inset, the prepared CD solution emitted bright green fluorescence under ultraviolet light. Furthermore, Fig. S1B (ESI†) reveals that with excitation wavelengths increasing from 380 to 440 nm, the green fluorescence emission peak position of the CD solution could be almost constant.

The fluorescence emission changes of CDs fabricated at different temperatures were also recorded (Fig. S2, ESI†). It was noted that the CD solution prepared at 180 °C had the optimal fluorescence emission signal. The morphology and size of CDs synthesized by the hydrothermal treatment of glucosamine and excess pyrophosphate were observed by TEM (Fig. S3A, ESI†). It was found that the generated CDs were near spherical with good dispersion and the size distribution gave an average size of 4.11 nm with ±1.23 nm. The FT-IR spectra were utilized to further confirm the chemical structure of the synthesized CDs. The broad O–H stretching vibration and absorption (3390 cm^{-1}, 1000 cm^{-1}), the stretching mode of C=O (1710 cm^{-1}), a pair of asymmetric and symmetric stretching modes of C–O–C (1340 cm^{-1}, 1180 cm^{-1}), the asymmetric stretching and deformational vibration of $-NH_2$ (3390 and 1660 cm^{-1}) and the absorption band of C–N (1300 cm^{-1}) were all observed in the FT-IR spectra of the CDs (Fig. S3B, ESI†). The presence of $-NH_2$ and C–N further indicated that the abundant $-NH_2$ group could remain at the surface of CDs even after the hydrothermal carbonization. Besides, the C=C stretching vibration in the CDs was observed at the absorption bands around 1590 cm^{-1}, 1510 cm^{-1} and 1380 cm^{-1}, which indicates that the surface of CDs was partially carbonized during the hydrothermal process.[21] Therefore, the obtained CDs were natural amino-functionalized green fluorescent CDs.

To further explore the potential applications of amino-functionalized CDs in biosensing, one of the primary requirements is water-solubility and stability under various pH and ionic environments. While CDs with abundant hydroxyl and amino groups were inherently water-soluble, their stability in various environments was further tested, as shown in Fig. S4 and S5 (ESI†). Fig. S4† indicates that the fluorescence intensity of the pre-prepared CD solution was almost the same in different pH environments, although a slight decrease was observed for the CDs with the pH environment of over 6.4. This is very different from many other water-soluble fluorescence dyes and quantum dots which usually exhibit obvious decrease in fluorescence emission with decreased pH values and poor fluorescence and stability in an acidic environment.[22] Moreover, some traditional dyes and quantum dots are faced with the interference from some ions and molecules such as Zn^{2+}, Fe^{3+} and L-cysteine (Cys).[23] As shown in Fig. S5,† we investigated the effect of various ions and molecules including K^+, Na^+, Ca^{2+}, Mg^{2+}, Zn^{2+}, Ni^{2+}, Fe^{3+}, Cu^{2+}, glucose (Glu), glycine (Gly), histidine (His) and Cys on the fluorescence of CDs. It was found that the CDs were also highly stable under various ionic and molecular environments. The high stability of CDs is a significant merit in sensing applications.

The SET system between CDs and HA-Au NPs

As shown in Fig. S6A (ESI†), the zeta potentials of amino-functionalized CD and HA-Au NP solution were determined to be +12.8 and −2.9 mV respectively. Therefore, the amino-functionalized CDs with a positive charge generated from protonated amine groups could attract HA-Au NPs with a negative charge by electrostatic interactions.[24] The TEM image further shows that some amino-functionalized CDs were distributed nearby HA-Au NPs in the mixture solution composed of CDs and HA-Au NPs (Fig. S6B, ESI†). It is well known that Au NPs exhibit efficiency in fluorescence quenching due to the non-radioactive electronic excitation energy transfer from the fluorescent probe to Au NPs.[25] The HA-Au NPs were prepared *via* the $NaBH_4$-reduction route, which offered the maximum absorption peak around 534 nm with a near spherical shape and a size centered at 22–27 nm (Fig. 3). It can be seen from Fig. 3A that there was a large overlap between the fluorescence emission spectra of the prepared amino-functionalized CDs and absorption spectra of HA-Au NPs. Therefore, we designed an efficient SET system between CDs and HA-Au NPs, and there was an obvious fluorescence quenching of CDs with the addition of HA-Au NPs (Fig. S7, ESI†). Moreover, the fluorescence lifetime of amino-functionalized CDs was determined to be 2.7 ns, and the fluorescence lifetime of the SET system

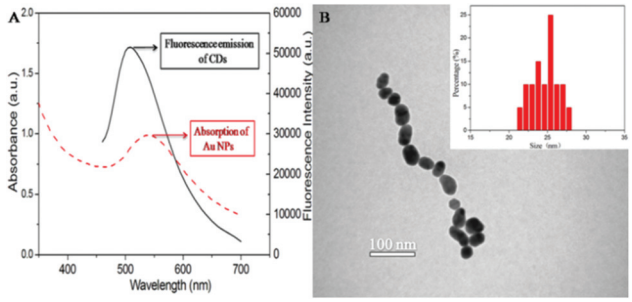

Fig. 3 (A) The fluorescence emission spectra of CD (solid line) and UV-Vis absorption spectra of HA-Au NP solution (dashed line). (B) The TEM image of HA-Au NPs.

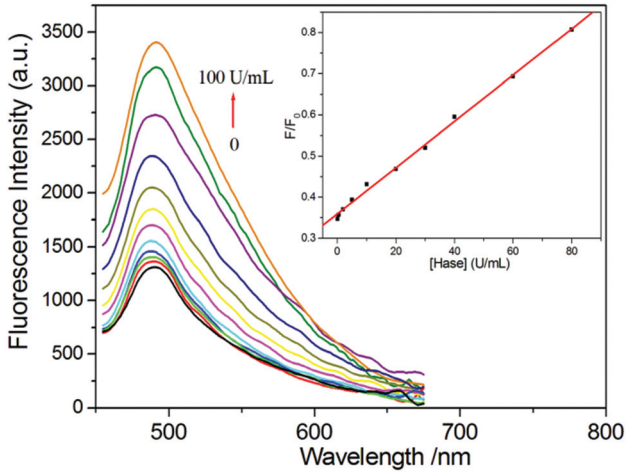

Fig. 4 Fluorescence spectra of the CD/HA-Au NP SET system incubated with different concentrations of Hase (0, 0.1, 0.5, 2, 5, 10, 20, 30, 40, 60, 80, 100 U mL^{-1}) for 2 hours. Inset shows the linear plots of F/F_0 *versus* the Hase concentration in the range of 0.1–80 U mL^{-1}. Reaction conditions: 10 mmol per L NaH_2PO_4–Na_2HPO_4 buffer solution (pH 6.0) at 37 °C.

composed of CDs and HA-Au NPs was 2.3 ns (Fig. S8, ESI†). With the addition of HA-Au NPs, the shorter lifetime from the SET system could help rule out the possibility of static quenching.

The SET system for detection of Hase

Hase, as a digesting endoglycosidase, can specially degrade linear HA molecules. We designed a detection strategy for Hase, as illustrated in Scheme 1B. HA molecules on the surface of Au NPs can effectively protect Au NPs and prevent aggregation. In the presence of enough Hase, HA molecules would decompose into low molecular weight fragments that lead to the aggregation and exit of Au NPs from the SET system. Fig. S9A (ESI†) displays the fluorescence signal changes of the CD/HA-Au NP SET system, with increasing Hase concentration (0–100 U mL^{-1}), incubated at different times (0–120 minutes). The fluorescence intensity increased gradually until the reaction time reached 120 minutes. Therefore 120 minutes of incubation time was used in further Hase assays. The color changes of the CD/HA-Au NP SET system in response to 100 U mL^{-1} Hase are shown in Fig. S9B.† Incubated with Hase for 2 hours, the CD/HA-Au NP solution changed from purple red into light red. Not only that, some black deposits could be observed at the bottom of CDs/HA-Au NPs incubated with Hase solution after low speed centrifugation, which visually indicated the generation of Au NP aggregation with enough Hase.

As shown in Fig. 4, the quenched fluorescence of CDs induced by HA-Au NPs was gradually recovered with the increase of Hase concentration that was caused by the aggregation of Au NPs and its exit from the SET system. Fig. 4 inset demonstrates that there is a good linear relationship between the relative fluorescence F/F_0 (F_0 is the original fluorescence intensity of CDs, and F is the fluorescence intensity of CDs/HA-Au NPs with the addition of various concentrations of Hase) and Hase concentrations in the range from 0.1 to 80 U mL^{-1}. The regression equation could be described as follows:

$$F/F_0 = 0.3593 + 0.0056[\text{Hase}], \text{U mL}^{-1} \quad (1)$$

The corresponding regression coefficient (R^2) is 0.998, and the detection limit for Hase is 0.06 U mL^{-1} calculated by following the 3σ IUPAC criteria. As shown in Fig. S10,† Hase and a series of proteins including bovine serum albumin (BSA), human serum albumin (HSA), bovine hemoglobin (HB), lysozyme (Lyz), trypsin (Try), and glutathione (GSH) were respectively added to the CD/HA-Au NP assay system to incubate for 120 minutes, and only Hase was able to effectively induce the fluorescence recovery of the assay solution due to its specific ability to degrade HA. Our proposed assay system yielded weak fluorescence responses to other proteins, which indicates that this strategy has high selectivity toward Hase.

In addition, Fig. 5A reveals that the absorption peak centered at 534 nm of the CD/HA-Au NP solution exhibited an

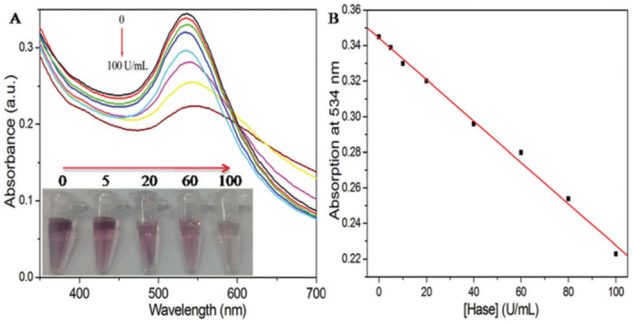

Fig. 5 (A) UV-Vis absorption spectra of the CD/HA-Au NP SET system incubated with different concentrations of Hase (0, 5, 10, 20, 40, 60, 80, 100 U mL^{-1}) for 2 hours. The inset picture shows the color change of the SET system solutions incubated with different concentrations of Hase (0, 5, 20, 60, 100 U mL^{-1}) for 2 hours. (B) The standard curve of absorbance at 534 nm as the function of Hase concentration (0, 5, 10, 20, 40, 60, 80, 100 U mL^{-1}). Reaction conditions: 10 mmol per L NaH_2PO_4–Na_2HPO_4 buffer solution (pH 6.0) at 37 °C.

obvious reduction with the increase of Hase concentration. At the same time, there was also a color change from purple red to light red, when incubated for 2 h, with the increase of Hase concentration in the assay system (Fig. 5A inset). Therefore, this assay offered a simple route for the quantitative estimation of Hase. Fig. 5B shows a standard curve in which the absorbance at 534 nm (A_{534}) of CD/HA-Au NP solution is plotted as a function of various Hase concentrations. The standard curve could be described as follows:

$$A_{534} = 0.3443 - 0.0012[\text{Hase}], \text{U mL}^{-1} \quad (2)$$

The corresponding regression coefficient R^2 was 0.996, and the detection limit for Hase was 1 U mL^{-1} with the dynamic range from 0 to 100 U mL^{-1}. Therefore, the Hase detection could be also performed using absorbance analysis besides fluorescence measurements.

Serum samples detection

In order to evaluate the feasibility of the proposed method in real sample detection, the developed detection system was applied for the determination of Hase in fetal bovine serum samples. The commercial fetal bovine serum was diluted 25 times with deionized water and then adjusted to pH 6.0. Different concentrations of Hase were added to the diluted serum samples to prepare the spiked samples. The results obtained by using the standard addition method are shown in Table S1,† and the accuracy of the proposed method was evaluated by determining the recovery of Hase in real samples. It can be seen that the recoveries in the real samples was between 102 and 108% and the RSD was not over 4.7%. The above results demonstrate the potential applicability of this method for the detection of Hase in serum samples.

Conclusion

In this study, for the first time, we have demonstrated that the highly fluorescent amino-functionalized CDs could be prepared by hydrothermal treatment of glucosamine with excess pyrophosphate. The amino-functionalized CDs offered constant green fluorescence emission at various excitation wavelengths and high stability when exposed to different pH and ionic environments. We further developed a facile SET assay system based on the amino-functionalized CDs and HA-Au NPs for the fluorescence detection of Hase. Moreover, the absorbance measurements could be conveniently used for quantitatively analysis of Hase based on the color change of the SET assay solution.

Acknowledgements

This work was supported by the Natural Science Foundation of China (81201141), the Fundamental Research Funds for Central Universities of China (N130520001), and the Liaoning Provincial Educational Commission (L2014095).

Notes and references

1 J. K. Jaiswal, H. Mattoussi, J. M. Mauro and S. M. Simon, *Nat. Biotechnol.*, 2003, **21**, 47.
2 X. Michalet, F. F. Pinaud, L. A. Bentolila, J. M. Tsay, S. Doose, J. J. Li, G. Sundaresan, A. M. Wu, S. S. Gambhir and S. Weiss, *Science*, 2005, **307**, 538.
3 C. Q. Ding, A. W. Zhu and Y. Tian, *Acc. Chem. Res.*, 2014, **47**, 20.
4 (*a*) J. H. Gao and B. Xu, *Nano Today*, 2009, **4**, 37; (*b*) X. Y. Li, H. Q. Wang, Y. Shimizu, A. Pyatenko, K. Kawaguchi and N. Koshizaki, *Chem. Commun.*, 2011, **47**, 932.
5 S. N. Baker and G. A. Baker, *Angew. Chem., Int. Ed.*, 2010, **49**, 6726.
6 Y. P. Sun, B. Zhou, Y. Lin, W. Wang, K. A. S. Fernando, P. Pathak, M. J. Meziani, B. A. Harruff, X. Wang, H. F. Wang, P. J. G. Luo, H. Yang, M. E. Kose, B. L. Chen, L. M. Veca and S. Y. Xie, *J. Am. Chem. Soc.*, 2006, **128**, 7756.
7 (*a*) L. Y. Zheng, Y. W. Chi, Y. Q. Dong, J. P. Lin and B. B. Wang, *J. Am. Chem. Soc.*, 2009, **131**, 4564; (*b*) S. T. Yang, L. Cao, P. G. Luo, F. S. Lu, X. Wang, H. F. Wang, M. J. Meziani, Y. F. Liu, G. Qi and Y. P. Sun, *J. Am. Chem. Soc.*, 2009, **131**, 11308; (*c*) Z. A. Qiao, Y. F. Wang, Y. Gao, H. W. Li, Y. L. Liu and Q. S. Huo, *Chem. Commun.*, 2010, **46**, 8812–8814; (*d*) D. Y. Pan, J. C. Zhang, Z. Li and M. H. Wu, *Adv. Mater.*, 2010, **22**, 734.
8 (*a*) S. L. Hu, K. Y. Niu, J. Sun, J. Yang, N. Q. Zhao and X. W. Du, *J. Mater. Chem.*, 2009, **19**, 484; (*b*) L. Y. Zheng, Y. W. Chi, Y. Q. Dong, J. P. Lin and B. B. Wang, *J. Am. Chem. Soc.*, 2009, **131**, 4564; (*c*) V. N. Mochalin and Y. Gogotsi, *J. Am. Chem. Soc.*, 2009, **131**, 4594; (*d*) Z. A. Qiao, Y. F. Wang, Y. Gao, H. W. Li, Y. L. Liu and Q. S. Huo, *Chem. Commun.*, 2010, **46**, 8812.
9 (*a*) S. Chandra, P. Das, S. Bag and D. Laha, *Nanoscale*, 2011, **3**, 1533; (*b*) J. Hou, J. Yan, Q. Zhao, Y. Li, H. Ding and L. Ding, *Nanoscale*, 2013, **5**, 9558; (*c*) D. Y. Pan, J. C. Zhang, Z. Li, Z. W. Zhang, L. Guo and M. H. Wu, *J. Mater. Chem.*, 2011, **21**, 3565; (*d*) H. Peng and J. Travas–Sejdic, *Chem. Mater.*, 2009, **21**, 5563.
10 (*a*) C. M. Lee, H. J. Jong, S. L. Kim, E. M. Kim, D. W. Kim, S. T. Lim, K. Y. Jang, Y. Y. Jeon, J. W. Nah and M. H. Sohn, *Int. J. Pharm.*, 2009, **371**, 163; (*b*) Z. A. Qiao, Y. F. Wang, Y. Gao, H. W. Li, T. Y. Dai, Y. L. Liu and Q. S. Huo, *Chem. Commun.*, 2010, **46**, 8812; (*c*) Y. H. Yang, J. H. Cui, M. T. Zheng, C. F. Hu, S. Z. Tan, Y. Xiao, Q. Yang and Y. L. Liu, *Chem. Commun.*, 2012, **48**, 380.
11 (*a*) M. W. Kramer, D. O. Escudero, S. D. Lokeshwar, R. Golshani, O. O. Ekwenna, K. Acosta, A. S. Merseburger, M. Soloway and V. B. Lokeshwar, *Cancer*, 2011, **117**, 1197; (*b*) C. J. Whatcott, H. Y. Han, R. G. Posner, G. Hostetter and D. D. Von-Hoff, *Cancer Discovery*, 2011, **1**, 291.
12 (*a*) H. F. Xie, F. Zeng and S. Z. Wu, *Biomacromolecules*, 2014, **15**, 3383; (*b*) V. B. Lokeshwar, V. Estrella, L. Lopez, M. Kramer, P. Gomez, M. S. Soloway and B. L. Lokeshwar, *Cancer Res.*, 2006, **66**, 11219; (*c*) J. J. Roberts, R. M. Elder,

A. Jayaraman and S. J. Bryant, *Biomacromolecules*, 2014, **15**, 1132.

13 (*a*) S. Eissa, M. Swellam, H. Shehata, I. El-Khouly, T. El-Zayat and O. El-Ahmady, *J. Urol.*, 2010, **183**, 493; (*b*) V. B. Lokeshwar, D. Rubinowicz, G. L. Chroeder, E. Forgacs, J. D. Minna, N. L. Block, M. Nadji and B. L. Lokeshwar, *J. Biol. Chem.*, 2001, **276**, 11922.

14 (*a*) R. Jin, L. S. M. Teixeira, P. J. Dijkstra, C. A. van Blitterswijk, M. Karperien and J. Feijen, *Biomaterials*, 2010, **31**, 3103; (*b*) S. W. Liao, T. B. Yu and Z. B. Guan, *J. Am. Chem. Soc.*, 2009, **131**, 17638.

15 (*a*) R. Chib, S. Raut, R. Fudala, A. Chang, M. Mummert, R. Rich, Z. Gryczynski and I. Gryczynski, *Curr. Pharm. Biotechnol.*, 2013, **14**, 470; (*b*) R. Fudala, M. E. Mummert, Z. Gryczynski and I. Gryczynski, *J. Photochem. Photobiol., B*, 2011, **104**, 473; (*c*) L. S. Zhang and M. E. Mummert, *Anal. Biochem.*, 2008, **379**, 80; (*d*) R. Fudala, M. E. Mummert, Z. Gryczynski, R. Rich, J. L. Borejdo and I. Gryczynski, *J. Photochem. Photobiol., B*, 2012, **106**, 69.

16 (*a*) S. Liu, J. Q. Tian, L. Wang, Y. W. Zhang, X. Y. Qin, Y. L. Luo, A. M. Asiri, A. O. Al-Youbi and X. P. Sun, *Adv. Mater.*, 2012, **24**, 2037; (*b*) W. B. Lu, X. Y. Qin, S. Liu, G. H. Chang, Y. W. Zhang, Y. L. Luo, A. M. Asiri, A. O. Al-Youbi and X. P. Sun, *Anal. Chem.*, 2012, **84**, 5351; (*c*) L. Zhou, Y. H. Lin, Z. Z. Huang, J. S. Ren and X. G. Qu, *Chem. Commun.*, 2012, **48**, 1147.

17 (*a*) P. C. Hsu, Z. Y. Shih, C. H. Lee and H. T. Chang, *Green Chem.*, 2012, **14**, 917; (*b*) X. F. Jia, J. Li and E. K. Wang, *Nanoscale*, 2012, **4**, 5572; (*c*) W. B. Shi, Q. L. Wang, Y. J. Long, Z. L. Cheng, S. H. Chen, H. Z. Zheng and Y. M. Huang, *Chem. Commun.*, 2011, **47**, 6695.

18 (*a*) J. M. Liu, J. T. Chen and X. P. Yan, *Anal. Chem.*, 2013, **85**, 3238; (*b*) P. K. Jain, X. H. Huang, I. H. El-Sayed and M. A. El-Sayed, *Acc. Chem. Res.*, 2008, **41**, 1578; (*c*) C. W. Chen, C. H. Wang, C. M. Wei, C. Y. Hsieh, Y. T. Chen, Y. F. Chen, C. W. Lai, C. L. Liu, C. C. Hsieh and P. T. Chou, *J. Phys. Chem. C*, 2009, **114**, 799; (*d*) D. Cheng, W. Y. Han, K. C. Yang, Y. Song, M. D. Jiang and E. Q. Song, *Talanta*, 2014, **130**, 408.

19 E. Q. Song, J. R. Li, H. Wei and Y. Song, *Anal. Methods*, 2012, **4**, 1199.

20 (*a*) R. E. Bailey and S. Nie, *J. Am. Chem. Soc.*, 2003, **125**, 7100; (*b*) R. Demir-Cakan, N. Baccile, M. Antonietti and M. M. Titirici, *Chem. Mater.*, 2009, **21**, 484.

21 (*a*) S. Chandra, P. Das, S. Bag and D. Laha, *Nanoscale*, 2011, **3**, 1533; (*b*) X. H. Wang, K. G. Qu, B. L. Xu, J. S. Ren and X. G. Qu, *J. Mater. Chem.*, 2011, **21**, 2445.

22 (*a*) C. P. Huang, Y. K. Li and T. M. Chen, *Biosens. Bioelectron.*, 2007, **22**, 1835; (*b*) A. Orte, J. M. Alvarez-Pez and M. J. Ruedas-Rama, *ACS Nano*, 2013, **7**, 6387; (*c*) A. M. Dennis, W. J. Rhee, D. Sotto, S. N. Dublin and G. Bao, *ACS Nano*, 2012, **6**, 2917.

23 (*a*) Y. F. Chen and Z. Rosenzweig, *Anal. Chem.*, 2002, **74**, 5132; (*b*) S. Huang, Q. Xiao, R. Li, H. L. Guan, J. Liu, X. R. Liu, Z. K. He and Y. Liu, *Anal. Chim. Acta*, 2009, **645**, 73.

24 (*a*) C. Carrillo-Carrió n, S. Cárdenas, B. M. Simonet and M. Valcárcel, *Anal. Chem.*, 2009, **81**, 4730; (*b*) W. Tedsana, T. Tuntulani and W. Ngeontae, *Anal. Chim. Acta*, 2013, **783**, 65.

25 (*a*) J. M. Liu, J. T. Chen and X. P. Yan, *Anal. Chem.*, 2013, **85**, 3238; (*b*) M. C. Daniel and D. Astruc, *Chem. Rev.*, 2004, **104**, 293.

